Dielectric Properties of GNPs@MgO/CuO@PVDF Composite Films

Safa POLAT *1

*1 Karabuk University, Material Research and Development Centre, KARABUK

(Alınış / Received: 05.08.2021, Kabul / Accepted: 02.11.2021, Online Yayınlanma / Published Online: 30.12.2021)

Keywords
MgO/CuO,
Graphene,
Composite film,
Dielectric constant

Abstract: In this study, it is aimed to develop dielectric materials with high dielectric coefficient for flexible capacitors. For this purpose, MgO/CuO nanoparticles were first synthesized by precipitation reactions. Then, these particles were added together with graphene nanoplates (GNPs) into PVDF in different compositions to form a composite mixture. After this process, flexible composite films of 30 µm thickness were formed with doctor blade and phase inversion methods. In the characterization processes, it was determined that MgO/CuO particles were successfully produced with an average size of 282 nm. On the other hand, the highest capacitance and dielectric coefficient values of the composite films were determined in the GNPs@MgO/CuO@PVDF sample as 2.8 nF and 42.6 at 100 Hz frequency, respectively. As a result, it was concluded that the dielectric properties were significantly improved with the use of graphene and metal oxides together, and PVDF was very successful in terms of flexibility and binding role.

GNPs@MgO/CuO@PVDF Kompozit Filmlerin Hazırlanması ve Dielektrik Özellikleri

Anahtar Kelimeler
MgO/CuO,
Grafen,
Kompozit film,
Dielektrik sabiti

Öz: Bu çalışmada, esnek kapasitörler için dielektrik katsayısı yüksek dielektrik malzemelerin geliştirilmesi amaçlanmıştır. Bu amaçla ilk olarak çöktürme reaksiyonları ile MgO/CuO nanopartikülleri sentezlenmiştir. Daha sonra bu partiküller grafen nanoplakaları (GNPs) ile birlikte PVDF içine farklı kompozisyonlarda eklenerek kompozit karışımı oluşturulmuştur. Bu işlemin ardından doktor blade ve phase inversion yöntemleri ile esnek yapılı 30 um kalınlığında kompozit filmler oluşturulmuştur. Karakterizasyon işlemlerinde MgO/CuO partiküllerinin ortalama 282 nm boyutunda başarılı bir şekilde üretildiği tespit edilmiştir. Öte yandan kompozit filmlerden en yüksek kapasitans ve dielektrik katsayısı değerleri 100 Hz. frekansta sırasıyla 2,8 nF ve 42,6 olarak GNPs@MgO/CuO@PVDF numunesinde tespit edilmiştir. Sonuç olarak grafen ve metal oksitlerin birlikte kullanımı ile dielektrik özellikler önemli ölçüde geliştirildiği ve ayrıca PVDF'in esneklik ve bağlayıcılık rolü bakımından oldukça başarılı olduğu sonucuna varılmıştır.

***Corresponding Author, e-mail:** safapolat@karabuk.edu.tr

1. Introduction

The concept of energy has been one of the important research topics in almost all disciplines from past to present. With the increase in the global population and the decrease in natural resources, it has begun to be investigated in a concrete sense. In these studies, importance was given to the use of renewable resources without harming the nature. In this context, energy production studies have been carried out so far by utilizing resources such as wind [1], solar [2], hydrothermal [3], geothermal and biomass [4]. In fact, electrical energies obtained from these sources are widely used in many areas of our daily lives. However, as an alternative to these energy sources, triboelectric nanogenerators (TENGs) have been developed in recent years to provide the energy of electronic devices such as watches and phones from daily activities [5,6]. TENGs have been developed to generate electricity from residual mechanical movements in our daily lives such as hand-arm movement, walking and running. The working principle of these devices is based on the principle of placing an insulating material on two conductor surfaces and rubbing them with each other [7]. Many studies have been carried out on this method for both application and material development in order to achieve higher output [8]. In these studies, it was stated that the use of materials with high dielectric coefficient increased the polarization and caused more electrification, which resulted in higher voltage outputs [9]. In terms of application, it has been aimed to develop flexible materials due to the human movement of the source [10]. On the other hand, there is no stable power output as sources like TENGs actually convert kinetic energy into electricity through motion in nature [11]. Therefore, it is also very important not only to obtain energy, but also to store it and make it available with appropriate outputs when needed. In this respect, the development of flexible capacitors and supercapacitors has been an intense research topic [12]. From these studies, it was concluded that it is a common requirement for the material to be developed for both cases to be flexible and have a high dielectric constant. Apart from these, it is known that flexible and high dielectric coefficient materials are also needed in biotechnological fields such as biosensor construction.

In this regard, when the studies done so far are examined, it has been observed that polymers such as poly-vinylidene fluoride (PVDF), Polyvinylpyrrolidone (PVP), polyimide (PI), polyvinylchloride (PVC), fluorinated ethylene propylene (FEP), and polytetrafluoroethylene (PTFE) are widely used [13–15]. Among these, PVDF is the polymer preferred in new generation piezoelectric material applications due to its easy workability, high temperature resistance, flame retardant feature, resistance to chemicals, abrasion, UV radiation, flexibility, low production cost and non-toxicity [16–21]. In particular, many studies have been carried out that it can be used in power microelectromechanical systems, wireless sensor networks, micro robots and implantable biological devices [22–25]. However, the fact that the piezoelectric charge constant values are not at the desired levels has brought some restrictions to the use of this material [26]. PVDF polymer, as it is commonly known, is a semi-crystalline polymer with five different crystal structures (α, β, γ, δ and ε). Among them, the alpha phase is the most common and has the highest thermal stability, while the beta phase is the most important in terms of piezoelectric and pyroelectric properties. Therefore, the conversion of the most concentrated alpha to the beta phase is actually the most necessary issue to increase the dielectric property of the polymer [23,24,27,28]. Various methods such as mechanical stretching, heat treatment application, casting with a solvent mixture have been used in order to achieve this [29–31]. Apart from these, another method especially used to increase the beta phase is to add nanoparticles to the polymer. It is known that various nanoparticles such as graphene [32], graphene oxide [33], carbon nanotube [34] and carbon black [35] have been used in studies carried out so far. In addition to these, it is known that many metal oxide materials have been used as an additive in polymers due to their superior dielectric properties due to their easy polarization [36–38]. In this context, structures such as MgO and CuO have been widely used in different applications [39–43]. However, it is observed that there is a lack in the literature on detailed investigations of these structures that can be obtained from chlorinated compounds of easily obtainable and very low-cost Mg and Cu elements. Therefore, this deficiency can be eliminated by making investigations with low cost 2A group and transition metals

In this study, it is aimed to develop composite films with high dielectric constant that can be used for new generation devices with flexible structure. For this purpose, firstly, MgO/CuO was synthesized from $MgCl_2$ and $CuCl_2$ metal oxides. Then, this structure was added to PVDF together with graphene and mixed homogeneously. When the mixture became muddy, it was plastered on a plate with the doctor blade method and then composite films were obtained by phase inversion method. First of all, the synthesized metal oxides and films were characterized by FTIR, XRD and SEM, and then the capacitance and dielectric coefficients were determined with an LCR meter. According to the final result, it was understood that the effect of the MgO/CuO structure alone was quite low, but it showed a high level of performance together with graphene.

2. Material and Method

2.1. Materials

$MgCl_2$, $CuCl_2$ salts and NaOH purchased from Aromel Kimya medical A.Ş were used for the synthesis MgO/CuO structure. Polyvinylene fluoride (PVDF) polymer used as binder was purchased in bulk form from Kahvecioğlu plastic and its solvent dimethyl formamide (DMF) was purchased from Aromel Kimya. Graphene was obtained from the company Nanografi. Production, measurements and use of various laboratory equipment such as pure water, beaker, and high temperature furnace were carried out in Karabuk University Materials Research and Development (MARGEM) laboratories.

2.2. Production method of MgO/CuO perovskit structure

For the synthesis of MgO/CuO structure, 13 mg of $MgCl_2$ and 11 mg of $CuCl_2$ salts were first dissolved in 50 ml of distilled water. Then, 22 mg of NaOH were added so that both of these salts were precipitated in the hydroxide structure and dissolved in 50 ml of distilled water in another beaker and transferred to the burette. Then the NaOH solution was started to be dripped into the metal chloride solution. The drip rate was set at such a rate that the entire solution would be finished in one hour. The obtained mixture was then filtered on watman filter paper, and the residues were thoroughly washed several times with distilled water. It was dried in an oven at 70 °C for about one day, along with the residues on the filter paper. The residues were then transferred to an alumina crucible and calcined in muffle furnace at 700 °C for 2 hours. This last process was carried out to break the O-H bonds and obtain the MgO/CuO structure. After this process, MgO/CuO powder was transferred to a mortar, where they were ground and made ready for use in composites. This production was repeated several times in order to produce enough MgO/CuO for all compositions.

2.3. Production of Composite films

For the production of composite films, first 50 mg of PVDF, 60 mg of active ingredient, 10 mg of graphene nanoplates (GNPs) and 2 ml of DMF were added to a beaker and mixed on a magnetic stirrer at 100 °C. After the PVDF was dissolved in DMF, mixing was continued until it reached a gel consistency. In the meantime, the aluminium foil was taped from the edges on a 15x15 cm glass. The surface of the foil was thoroughly cleaned with ethyl alcohol so that there were no wrinkles on the surface. Then, the mixture, which came to a gel consistency, was poured on the foil, and plastered on the surface with the doctor blade method. After this process, the glass and foil were immersed in a water-filled container and the active substance plastered on the surface was removed as a film on the water surface. With this method, all productions were carried out in the compositions given in Table 1. The intended material was obtained by drying the composite films in an oven at 70 °C for about one hour on the watch glass.

Table 1.

Sample	PVDF	MgO/CuO	GNP
#1	50 mg	-	-
#2	50 mg	30+30 mg	-
#3	50 mg	-	10 mg
#4	50 mg	30+30 mg	10 mg

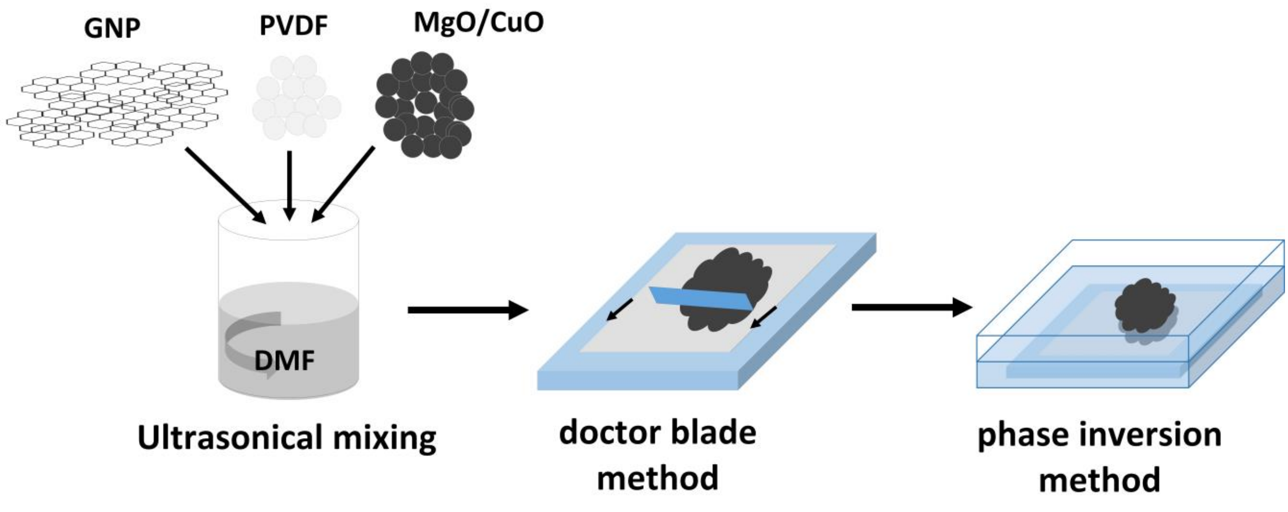

Figure 1. Representation images of experimental methods

2.4. Characterization of Materials

In this part of the study, firstly, the characterization of the MgO/CuO compounds, which was synthesized, was carried out. For this, chemical bond characterizations with FTIR, crystal structure analysis with XRD and particle size analysis with SEM were performed. Afterwards, FTIR, XRD and SEM analysis of the composite films were performed, and the final composites were characterized in terms of their components and interactions. Apart from these, in order to examine the dielectric properties, the films poured on the aluminium foil were dried there, and a 15x15 mm metal plate was contacted on it. In this process, first the capacitance values (C) of the composite films were measured with the LCR meter, and then the dielectric constants were calculated according to the formula in equation 1 [44].

$$C = \varepsilon_0 \varepsilon_r A/t \qquad (1)$$

Where ε_0 is the dielectric constant of the free space (8.854×10^{-12} F/m), ε_r is dielectric constant, A is area (m^2), and t is thickness (m) of the composites.

3. Results

XRD analysis was first performed to characterize the products obtained after the productions. In this analysis, MgO+CuO synthesis nanopowder were first analysed and then the composites of these powders combined with GNP and PVDF were analysed. The results obtained are detailed in Fig. 2. According to the results obtained, two sharp and high-intensity peaks were observed at approximately 32° and 39° with the 2θ value. These peaks belong to the (110) and (200) planes of CuO, respectively [45]. Apart from these, the peaks observed with lower intensity at 49°, 53°, 58°, 61°, 66°, 68°, 72° and 75° also indicate CuO (-202), (020), (202), (-113), (022), (-311), (220), (311) and (004) planes. Peaks belonging to MgO were observed at approximately 37°, 43°, 62°, 74° and 79° [46]. These peaks belong to the (111), (200), (220), (311) and (222) planes of MgO [47]. Apart from these, very low-intensity peaks observed also belong to CuO and MgO, but only sharp and intense ones were characterized. According to these results, XRD analysis show that it can be said that the synthesized powders are completely composed of CuO and MgO and no extra crystals are formed. Another analysis made with XRD is the composites of these powders combined with GNPs and PVDF. As a result of this analysis, the presence of GNPs in the composite was tried to be confirmed. According to the result given in a small graph embedded in the graph, it can be said that the peak observed at approximately 29° belongs to the (002) plane of the graphene [48]. However, while this peak should have been observed around 27°, it is thought that a shift of about 2° occurred and this was due to other crystals in the composite.

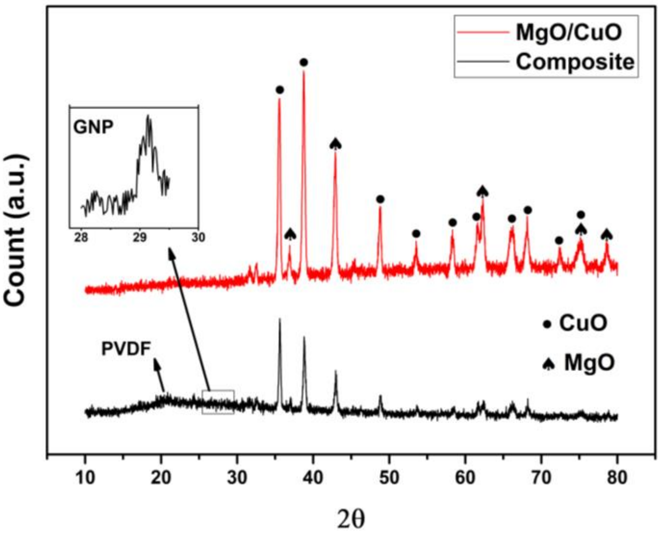

Figure 2. XRD results of composite films and MgO/CuO nanoparticles

FTIR analysis was carried out to confirm the accuracy of the crystal structures by chemical bonding between atoms. The results obtained are given in Fig. 3 in detail. According to these results, the peaks observed at approximately 2980 and 3020 cm^{-1} in wavenumber are due to the symmetrical and asymmetric stretching of $-CH_2$ [49]. Apart from these, more characteristic and sharp peaks of PVDF were also observed. One of them is the peak caused by the asymmetric and symmetrical $-CF_2$ tension observed at 1167 cm^{-1} [50]. On the other hand, it is known that PVDF contains alpha and beta phases. Approximately 1401, 1230, 1067, 875 and 834 cm^{-1} of these peaks indicate the vibration of the beta phase [50]. The low intensity peak observed at 764 cm^{-1} corresponds to the alpha phase [50]. The disappearance of this peak in composites actually means that the alpha phase has undergone transformation. However, the presence of beta phase peaks in composites means that PVDF protects its main skeleton without reacting with externally added components. Slight shifts were observed in the intensity and location of these peaks in the composites, which is thought to be due to the presence of different components. As for the synthesized metal oxide nanopowder, the peaks observed at 471, 574 and 642 cm^{-1} are due to the vibration of the Cu-O bond [51]. In addition, one of the broad peaks observed around 570 (561 cm^{-1}) is attributed to the vibration of Mg-O [52]. Based on these results, it can be said that both metal oxides and composites were synthesized and produced for the desired purposes.

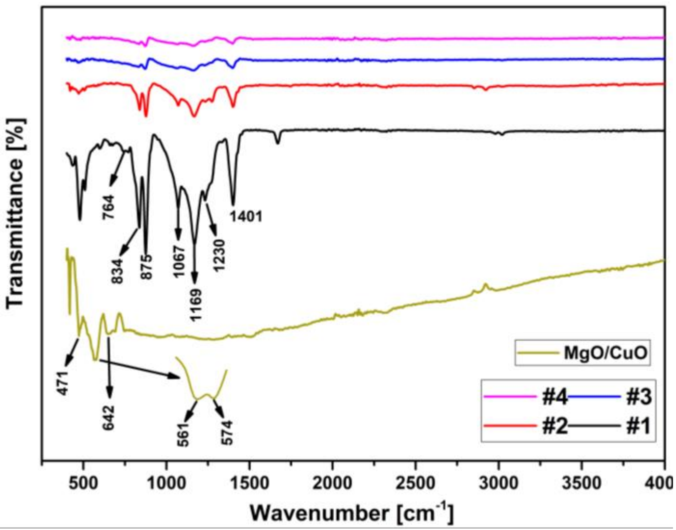

Figure 3. FTIR spectrums of composite films and MgO/CuO nanoparticles

Microstructure investigations of the synthesized MgO/CuO nanopowder were carried out by SEM and the results are given in figure 4 in detail. According to these results, the synthesized particles are mostly spherical in shape. However, spherical particles differ in size. All these particles are in contact with each other and show a homogeneous distribution. ImageJ program was used to determine the particle size distribution and average size. According to the results given in Figure 4b, the particle size generally varies between 100 nm and 600 nm, with an average size of 282 nm. About 5% of them are around 100 nm, 20% are 150-250 nm, 25% are 250-300 nm, and most of the rest is 300-450 nm. Apart from these, about 5% of them are around 500-600 nm. Almost all these particles have the same particle shape, indicating that both CuO and MgO occur in similar structures. This is thought to be since it was synthesized in the same environment and under the same conditions. On the other hand, the mapping images in figures 4c and d show a homogeneous distribution of copper and magnesium. This situation shows that both copper and magnesium oxide are synthesized in an intertwined manner. As a result, in this study, it can be said that the synthesis of nanoscale CuO and MgO was successfully synthesized at nanoscale by making a homogeneous attempt.

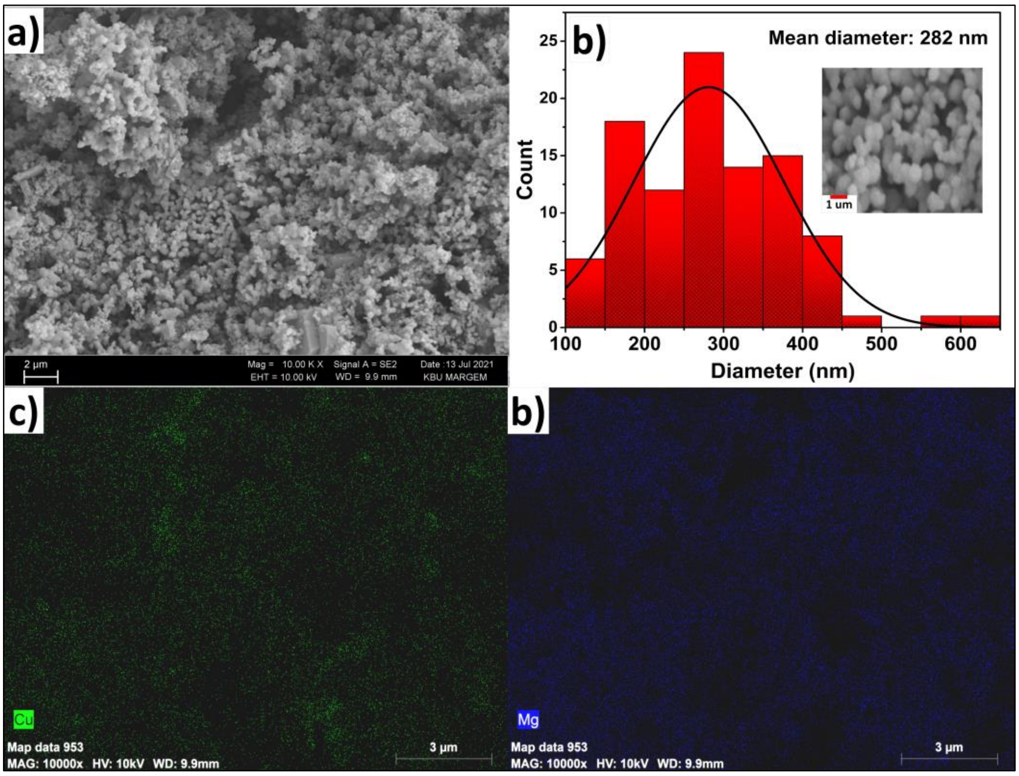

Figure 4. a) SEM images of MgO/CuO, b) histogram graph of particle diameter of MgO/CuO with inset images, c and d) mapping images of MgO/CuO nanoparticles

On the other hand, the digital image and SEM images of the composite film of sample #4 are given in figure 5 as a representation. According to these images, it is understood that the composite film has a very flexible structure. On the other hand, in the SEM image, it is seen that the spherical MgO/CuO particles are homogeneously dispersed in the PVDF. The smaller particles in these images are graphene nanoplates. In these images, there are also interparticle spaces called porosity. These are thought to be due to the increase in viscosity with the addition of particles into PVDF during production. It is also thought that it may be due to shrinkage of PVDF during drying. As a result, it can be said that composite films with flexible structure and homogeneous distribution of particles are successfully produced by the methods used.

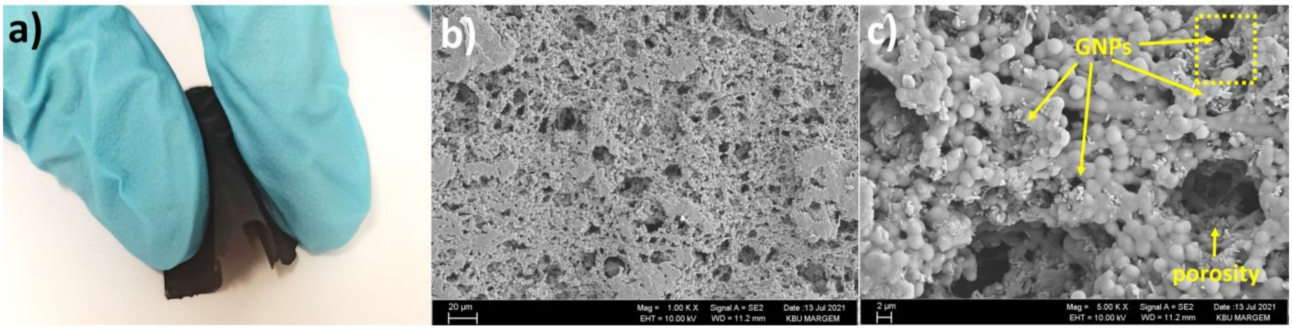

Figure 5. a) Digital images of flexible composite film (#4), b-c) SEM images of composite film (#4) at different magnifications

In order to determine the energy storage capacity of composite films, capacitance measurements were made with LCR meters and dielectric coefficients were determined accordingly. The obtained results were detailed in figure 6. According to these results, the capacitance values of the composite films at 100 Hz frequency were measured as 140 pF for the undoped PVDF film (#1), 203 pF for the MgO/CuO doped film (#2), 1555 pF for the graphene doped film (#3) and 2829 pF for the MgO/CuO and graphene doped film. When the frequency was increased to 1 kHz, the capacitance value was measured as 122 pF in sample #1, 157 pF in sample #2, 778 pF in sample #3 and 1059 pF in sample #4. When the frequency value was increased to 100 kHz, the capacitance values of these samples were measured as 109 pF, 114 pF, 316 pF and 365 pF, respectively.

On the other hand, dielectric coefficient values at 100 Hz were measured as 2.11 for #1 sample, 3.06 for #2 sample, 23.4 for #3 and 42.6 for #4. These results were measured to be 1.84, 2.37, 11.7 and 16 samples #1-#2-#3-#4 when the frequency value was increased to 1 kHz. When the frequency value was increased to 100 kHz, the same samples were measured as 1.64, 1.72, 4.76 and 5.5, respectively. According to these results, it was understood that the samples with the highest dielectric coefficient values were obtained in #3 and #4 samples and at low frequencies. In other words, it has been understood that when the synthesized metal oxides are used alone, the dielectric coefficient of pure PVDF relatively increases, but when it is used together with graphene, it provides a superior increase with a synergistic effect. It is an undeniable fact that graphene made the biggest contribution to this increase. Likewise, this situation has been proven in many articles in the literature. However, the dielectric constant value provided by graphene alone is lower than that provided by the metal oxide combination. Therefore, the composition of the components that make up sample #4 is considerable. Therefore, the energy storage capacity of this sample is higher than the highest values of other samples, even at high frequencies. For example, sample #4's capacitance values at 100 Hz and 1kHz are about 1.6 nF and 2.8 nF, while sample #3's capacitance is only around 1.6 nF at 100 Hz. Based on these results, it can be said that sample #4 can be used both in triboelectric nanogenerators and in other fields due to its flexible structure and high capacitance value. It can also be said that sample #3 can also be used in this context due to its relatively high capacitance value.

When it comes to the analysis of these results depending on the frequency variable, it is clearly understood that as the frequency increases, the capacitance and the dielectric coefficient values related to it decrease. In this context, it is known that electron jumps occur faster at low frequencies, which causes the polarization to increase rapidly. [53,54]. However, at high frequencies, the relaxation time of the charge carrier is not as fast as the change of the electric field over time, and this causes a decrease in capacitance [53]. Therefore, it can be said that higher capacitance values are achieved at higher frequencies. On the other hand, when it comes to evaluating the amount of supplements, Rozana et al. added 5% MgO to PVDF and measured ε_r value of around 5 at 10^4 Hz. [55]. Similarly, Chen et al., determined ε_r value around 9 with 4% reinforcement at the same frequency [56]. The results of this study are quite behind when only MgO supplementation is considered compared to the literature data. However, the high amount of additives in this study brought along porosity and agglomeration, which are the most important parameters that negatively affect the dielectric coefficient [57]. On the other hand, Rani et al., measured ε_r value as 6.6 at 100 Hz by adding 0.5% GNP and 5% CuO to the PVDF/PEDOT-block-PEG mixture, while adding 2.5% GNP and 25% CuO, they measured 34 [45]. In addition, in another study, the dielectric coefficient was around 20 when 10% by weight graphene was added to a mixture of polystyrene (PS) and polyvinylidene fluoride (PVDF), but this value reached up to 100 when the graphene amount was increased to 15% [58]. Based on these results, it is seen that if the metal oxide ratio is used at a high rate, it reduces ε_r value, but if it is used with graphene at a high rate, it has a synergistic effect and provides a higher increase than expected. The reason for this is understood in the BN-ZnO-GNP study that nano-sized plate-shaped graphene structures provide very high capacitance by forming many serial and parallel nano cells with metal oxide and PVDF dielectrics in the composite [54]. As a result, the obtaining of different types of composites by combining graphene with various metal oxides is very promising in terms of obtaining high dielectric constant materials.

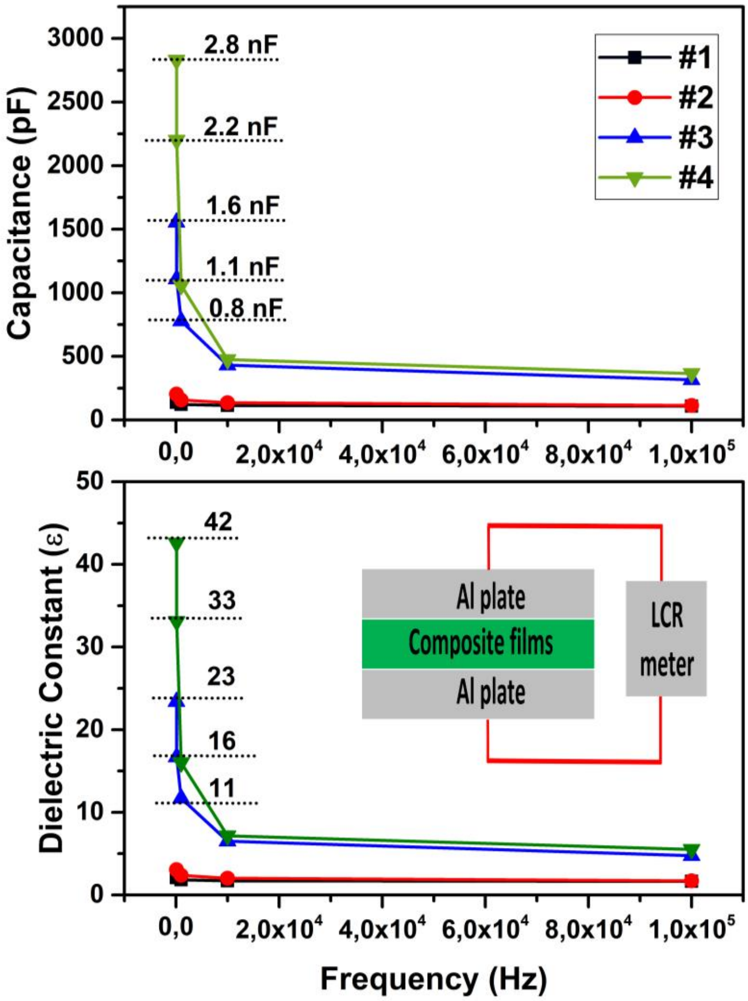

Figure 6. Frequency dependent changes of capacitance and dielectric constant values

4. Discussion and Conclusion

In this study, it is aimed to develop dielectric materials of flexible capacitors in order to increase the energy storage capacity of new generation flexible electronic devices. For this purpose, firstly, MgO/CuO nanoparticles were synthesized by precipitation reactions and calcination process. Then, composite mixture was formed by adding these nanoparticles together with graphene into PVDF in different compositions. Afterwards, composite films were successfully produced with doctor blade and phase inversion methods. In the characterization processes, it was understood that MgO/CuO particles were successfully produced with an average size of 282 nm. PVDF-based flexible composites have been successfully produced by applying the methods together. In the capacitance and dielectric constant measurements, the highest values were determined as 2.8 nF and 42.6 at 100 Hz, respectively. According to these results, it can be said that #4 is promising for new generation electronic devices in terms of both its flexible structure and high capacitance value.

Acknowledgment

This study was supported within the scope of the project numbered "KBÜBAP-21-ABP-047" supported by the Scientific Research Projects Coordination Unit of Karabuk University. In addition, Karabuk University MARGEM laboratories were used. We thank both departments for supporting the study.

References

[1] Sahin AD. Progress and recent trends in wind energy. Progress in Energy and Combustion Science 2004;30:501–43.

[2] López CSP, Frontini F. Energy efficiency and renewable solar energy integration in heritage historic buildings. Energy Procedia 2014;48:1493–502.

[3] Sharma HB, Sarmah AK, Dubey B. Hydrothermal carbonization of renewable waste biomass for solid biofuel production: A discussion on process mechanism, the influence of process parameters, environmental performance and fuel properties of hydrochar. Renewable and Sustainable Energy Reviews 2020;123:109761.

[4] Apergis N, Tsoumas C. Integration properties of disaggregated solar, geothermal and biomass energy consumption in the US. Energy Policy 2011;39:5474–9.

[5] Wang H, Wu T, Zeng Q, Lee C. A review and perspective for the development of triboelectric nanogenerator (TENG)-Based self-powered neuroprosthetics. Micromachines 2020;11:865.

[6] Ozen A, Ozel F, Kınas Z, Karabiber A, Polat S. Spring assisted triboelectric nanogenerator based on sepiolite doped polyacrylonitrile nanofibers. Sustainable Energy Technologies and Assessments 2021;47:101492.

[7] Kim W-G, Kim D-W, Tcho I-W, Kim J-K, Kim M-S, Choi Y-K. Triboelectric Nanogenerator: Structure, Mechanism, and Applications. ACS Nano 2021;15:258–87.

[8] Song Y, Shi Z, Hu G-H, Xiong C, Isogai A, Yang Q. Recent advances in cellulose-based piezoelectric and triboelectric nanogenerators for energy harvesting: a review. Journal of Materials Chemistry A 2021;9:1910–37.

[9] Zhu G, Peng B, Chen J, Jing Q, Lin Wang Z. Triboelectric nanogenerators as a new energy technology: From fundamentals, devices, to applications. Nano Energy 2015;14:126–38. https://doi.org/10.1016/j.nanoen.2014.11.050.

[10] Niu Z, Cheng W, Cao M, Wang D, Wang Q, Han J, et al. Recent Advances in Cellulose-Based Flexible Triboelectric Nanogenerators. Nano Energy 2021:106175.

[11] Wang ZL. Triboelectric Nanogenerators as New Energy Technology for Self-Powered Systems and as Active Mechanical and Chemical Sensors. ACS Nano 2013;7:9533–57. https://doi.org/10.1021/nn404614z.

[12] Liu M, Wang L, Yu X, Zhang H, Zhang H, Li S, et al. Introducing oxygen vacancies for improving the electrochemical performance of Co9S8@ NiCo-LDH nanotube arrays in flexible all-solid battery-capacitor hybrid supercapacitors. Energy 2022;238:121767.

[13] Yang J, Chen J, Yang Y, Zhang H, Yang W, Bai P, et al. Broadband vibrational energy harvesting based on a triboelectric nanogenerator. Advanced Energy Materials 2014;4:1301322.

[14] Zhang C, Zhou T, Tang W, Han C, Zhang L, Wang ZL. Rotating-disk-based direct-current triboelectric nanogenerator. Advanced Energy Materials 2014;4:1301798.

[15] Davies DK. Charge generation on dielectric surfaces. Journal of Physics D: Applied Physics 1969;2:1533.

[16] Laudari A, Barron J, Pickett A, Guha S. Tuning charge transport in PVDF-based organic ferroelectric transistors: Status and outlook. ACS Applied Materials & Interfaces 2020;12:26757–75.

[17] Holmes-Siedle AG, Wilson PD, Verrall AP. PVdF: An electronically-active polymer for industry. Materials & Design 1983;4:910–8.

[18] Foster FS, Harasiewicz KA, Sherar MD. A history of medical and biological imaging with polyvinylidene fluoride (PVDF) transducers. IEEE Transactions on Ultrasonics, Ferroelectrics, and Frequency Control 2000;47:1363–71.

[19] Chen S, Skordos A, Thakur VK. Functional nanocomposites for energy storage: Chemistry and new horizons. Materials Today Chemistry 2020;17:100304.

[20] Sessler GM. Piezoelectricity in polyvinylidenefluoride. The Journal of the Acoustical Society of America 1981;70:1596–608.

[21] Jain A, KJ P, Sharma AK, Jain A, PN R. Dielectric and piezoelectric properties of PVDF/PZT composites: A review. Polymer Engineering & Science 2015;55:1589–616.

[22] Proto A, Fida B, Bernabucci I, Bibbo D, Conforto S, Schmid M, et al. Wearable PVDF transducer for biomechanical energy harvesting and gait cycle detection. 2016 IEEE EMBS Conference on Biomedical Engineering and Sciences (IECBES), IEEE; 2016, p. 62–6.

[23] Zaccaria M, Fabiani D, Zucchelli A, Belcari J, Bocchi O. Vibration energy harvesting using electrospun nanofibrous PVdF-TrFE. 2016 IEEE international conference on dielectrics (ICD), vol. 2, IEEE; 2016, p. 796–9.

[24] Abolhasani MM, Shirvanimoghaddam K, Naebe M. PVDF/graphene composite nanofibers with enhanced piezoelectric performance for development of robust nanogenerators. Composites Science and Technology 2017;138:49–56.

[25] Liu W, Cheng X, Fu X, Stefanini C, Dario P. Preliminary study on development of PVDF nanofiber based energy harvesting device for an artery microrobot. Microelectronic Engineering 2011;88:2251–4. https://doi.org/10.1016/j.mee.2011.02.098.

[26] Cai J, Hu N, Wu L, Liu Y, Li Y, Ning H, et al. Preparing carbon black/graphene/PVDF-HFP hybrid composite films of high piezoelectricity for energy harvesting technology. Composites Part A: Applied Science and Manufacturing 2019;121:223–31. https://doi.org/10.1016/j.compositesa.2019.03.031.

[27] Liang C-L, Xie Q, Bao R-Y, Yang W, Xie B-H, Yang M-B. Induced formation of polar phases in poly (vinylidene fluoride) by cetyl trimethyl ammonium bromide. Journal of Materials Science 2014;49:4171–9.

[28] Ponnamma D, Erturk A, Parangusan H, Deshmukh K, Ahamed MB, Al Ali Al-Maadeed M. Stretchable quaternary phasic PVDF-HFP nanocomposite films containing graphene-titania-SrTiO3 for mechanical energy harvesting. Emergent Mater 2018;1:55–65. https://doi.org/10.1007/s42247-018-0007-z.

[29] Zhang Z, Cao M, Chen P, Yang B, Wu B, Miao J, et al. Improvement of the thermal/electrical conductivity of PA6/PVDF blends via selective MWCNTs-NH2 distribution at the interface. Materials & Design 2019;177:107835.

[30] Yun S, Kim J. Mechanical, electrical, piezoelectric and electro-active behavior of aligned multi-walled carbon nanotube/cellulose composites. Carbon 2011;49:518–27.

[31] Martins P, Lopes AC, Lanceros-Mendez S. Electroactive phases of poly (vinylidene fluoride): Determination, processing and applications. Progress in Polymer Science 2014;39:683–706.

[32] Cui L, Lu X, Chao D, Liu H, Li Y, Wang C. Graphene-based composite materials with high dielectric permittivity via an in situ reduction method. Physica Status Solidi (a) 2011;208:459–61.

[33] Sabira K, Saheeda P, Divyasree MC, Jayalekshmi S. Impressive nonlinear optical response exhibited by Poly (vinylidene fluoride)(PVDF)/reduced graphene oxide (RGO) nanocomposite films. Optics & Laser Technology 2017;97:77–83.

[34] Wu C-M, Chou M-H, Zeng W-Y. Piezoelectric response of aligned electrospun polyvinylidene fluoride/carbon nanotube nanofibrous membranes. Nanomaterials 2018;8:420.

[35] Doh C, Jin B, Moon S, Chung Y-D, Jeong D, Bang Y. Physical and Electrical Properties of Carbon Black/PVDF Composite Electrode as Ohmic Joule Heater. Applied Chemistry for Engineering 2009;20:692–5.

[36] Thakur VK, Gupta RK. Recent progress on ferroelectric polymer-based nanocomposites for high energy density capacitors: synthesis, dielectric properties, and future aspects. Chemical Reviews 2016;116:4260–317.

[37] Akinay Y, Kizilcay AO. Computation and modeling of microwave absorbing CuO/graphene nanocomposites. Polymer Composites 2020;41:227–32.

[38] Lunkenheimer P, Krohns S, Riegg S, Ebbinghaus SG, Reller A, Loidl A. Colossal dielectric constants in transition-metal oxides. The European Physical Journal Special Topics 2009;180:61–89.

[39] Jaschin PW, Bhimireddi R, Varma KBR. Enhanced Dielectric Properties of LaNiO3/BaTiO3/PVDF: A Three-Phase Percolative Polymer Nanocrystal Composite. ACS Appl Mater Interfaces 2018;10:27278–86. https://doi.org/10.1021/acsami.8b07786.

[40] Sarkar S, Jana PK, Chaudhuri BK, Sakata H. Copper (II) oxide as a giant dielectric material. Applied Physics Letters 2006;89:212905.

[41] Oruç Ç, Altındal A. Structural and dielectric properties of CuO nanoparticles. Ceramics International 2017;43:10708–14.

[42] Fang X-S, Ye C-H, Xie T, Wang Z-Y, Zhao J-W, Zhang L-D. Regular MgO nanoflowers and their enhanced dielectric responses. Applied Physics Letters 2006;88:013101.

[43] Lee SY, Tseng T-Y. Electrical and dielectric behavior of MgO doped Ba 0.7 Sr 0.3 TiO 3 thin films on Al 2 O 3 substrate. Applied Physics Letters 2002;80:1797–9.

[44] Rao JK, Raizada A, Ganguly D, Mankad MM, Satayanarayana SV, Madhu GM. Investigation of structural and electrical properties of novel CuO–PVA nanocomposite films. J Mater Sci 2015;50:7064–74. https://doi.org/10.1007/s10853-015-9261-0.

[45] Rani P, Basheer Ahamed M, Deshmukh K. Dielectric and electromagnetic interference shielding performance of graphene nanoplatelets and copper oxide nanoparticles reinforced polyvinylidenefluoride/poly(3,4-ethylenedioxythiophene)-block-poly (ethylene glycol) blend nanocomposites. Synthetic Metals 2021;282:116923. https://doi.org/10.1016/j.synthmet.2021.116923.

[46] Zhu D, Wang L, Yu W, Xie H. Intriguingly high thermal conductivity increment for CuO nanowires contained nanofluids with low viscosity. Scientific Reports 2018;8:1–12.

[47] Balakrishnan G, Velavan R, Batoo KM, Raslan EH. Microstructure, optical and photocatalytic properties of MgO nanoparticles. Results in Physics 2020;16:103013.

[48] Niftaliyeva A, Pehlivan E, Polat S, Avci A. Chemical synthesis of single-layer graphene by using ball milling compared with NaBH4 and hydroquinone reductants. Micro & Nano Letters 2018;13:1412–6.

[49] Mohamadi S. Preparation and Characterization of PVDF/PMMA/Graphene Polymer Blend Nanocomposites by Using ATR-FTIR Technique. IntechOpen; 2012. https://doi.org/10.5772/36497.

[50] Ji Y, Liu J, Jiang Y, Liu Y. Analysis of Raman and infrared spectra of poly(vinylidene fluoride) irradiated by KrF excimer laser. Spectrochimica Acta Part A: Molecular and Biomolecular Spectroscopy 2008;70:297–300. https://doi.org/10.1016/j.saa.2007.07.061.

[51] B. Tanvir N, Yurchenko O, Wilbertz C, Urban G. Investigation of CO 2 reaction with copper oxide nanoparticles for room temperature gas sensing. Journal of Materials Chemistry A 2016;4:5294–302. https://doi.org/10.1039/C5TA09089J.

[52] Kandiban M, Vigneshwaran P, Potheher I. SYNTHESIS AND CHARACTERIZATION OF MGO NANOPARTICLES FOR PHOTOCATALYTIC APPLICATIONS. 2015.

[53] Zhang SS. Dual-Carbon Lithium-Ion Capacitors: Principle, Materials, and Technologies. Batteries & Supercaps 2020.

[54] Polat S. Dielectric Properties of BN-ZnO-GNP Doped PU-EG Composites. International Journal of Engineering Research and Development 2021;13:635–44. https://doi.org/10.29137/umagd.896904.

[55] Arshad AN, Wahid MHM, Rusop M, Majid WHA, Subban RHY, Rozana MD. Dielectric and Structural Properties of Poly(vinylidene fluoride) (PVDF) and Poly(vinylidene fluoride-trifluoroethylene) (PVDF-TrFE) Filled with Magnesium Oxide Nanofillers. Journal of Nanomaterials 2019;2019:e5961563. https://doi.org/10.1155/2019/5961563.

[56] Chen S, Hu J, Gao L, Zhou Y, Peng S, He J, et al. Enhanced breakdown strength and energy density in PVDF nanocomposites with functionalized MgO nanoparticles. RSC Adv 2016;6:33599–605. https://doi.org/10.1039/C6RA01869F.

[57] Chu L, Xue Q, Sun J, Xia F, Xing W, Xia D, et al. Porous graphene sandwich/poly (vinylidene fluoride) composites with high dielectric properties. Composites Science and Technology 2013;86:70–5.

[58] Kumar NA, Ravibabu V, Ashokbabu A, Thomas P. Effect of Graphene Nanoplatelets (GNP) on the Dielectric and Thermal Properties of Polystyrene (PS)/Polyvinylidenedifluoride (PVDF) Blends. 2021 IEEE International Conference on the Properties and Applications of Dielectric Materials (ICPADM), IEEE; 2021, p. 354–7.